J Mater Sci: Mater Electron (2007) 18:805–810
DOI 10.1007/s10854-007-9210-z

Application of power loss calculation to estimate the specific contact resistance of the screen-printed silver ohmic contacts of the large area silicon solar cells

P. N. Vinod

Received: 27 June 2006 / Accepted: 20 February 2007 / Published online: 24 March 2007

Abstract The establishment of a suitable contact formation methodology is a critical part of the technological development of any metal-to-semiconductor contact structure. Many test structures and methodologies have been proposed to estimate the specific contact resistance (ρ_c) of the planar ohmic contacts formed on the heavily doped semiconductor surface. These test structures are usually processed on the same wafer to monitor a particular process. In this study, new experimental procedure has been evolved to assess the value of ρ_c of the screen-printed front silver (Ag) thick-film metal contact to the silicon surface. The essential feature of this methodology is that it is an iteration technique based on the calculation of power loss associated with various resistive components of the solar cell normalized to the unit cell area. Therefore, this method avoids the complexity of making the design of any lay out of a standard contact resistance test structure like transmission line model (TLM) or Kelvin resistor, etc. It was shown that value of specific contact resistance of the order of 1.0×10^{-5} Ω–cm^2 is measured for the Ag metal contacts formed on the n^+ silicon surface. This value is much lower than the ρ_c data previously reported for the screen-printed Ag contacts. The sintering process of the front metal contact structure at different furnace setting is carried out to understand the possible wet interaction and metal contact formation as a function of the firing. Therefore, the study is further extended to study the peak firing temperature dependence of the ρ_c of screen-printed Ag metal contacts. It will help to assess the specific contact resistance of the ohmic contacts as a function of firing temperature of sintering process.

P. N. Vinod (✉)
Naval Physical and Oceanographic Laboratory, Thrikkakara P.O, Cochin 682 021, India
e-mail: drpnvinod@yahoo.com

1 Introduction

Screen-printing techniques used in the solar cell manufacturing are applied for the industrial cost effective large area silicon solar cells. It consists of printing of thick film Ag conductor paste on the heavily doped n^+ silicon surface in a characteristic grid pattern to minimize the resistive and shadowing losses [1, 2]. The rear contact consists of fully covered aluminum containing silver (Al/Ag) contact metallization. It follows a sintering step at an elevated temperature under proper ambient conditions is applied to produce desired ohmic characteristics [2]. Therefore, formation of good electrical contacts and assessing its ohmic properties is considered as an important process in the device fabrication step. A useful approach to quantitatively assess the electrical nature of the ohmic contacts is to measure the value of the specific contact resistance ρ_c(Ω-cm^2). It was shown that the specific contact resistance is the parameter that characterizes the interfacial properties of the metal-to-semiconductor contact structure. This serves as a measure of the ohmic or rectifying behavior (non-ohmic Schottky barrier) of the metal-to-semiconductor barrier at the interface of the metal-to-semiconductor surface. As predicted by the transmission line model (TLM) [3], the barrier opposing the current flow between the metal and the semiconductor interface is characterized by a finite value of specific contact resistance, which under zero applied voltage is defined as [4],

$$\rho_c = \left|\frac{dJ}{dV}\right|^{-1}_{V=0} \quad (1)$$

where J is current density across the metal-to-semiconductor interface and V is the applied voltage across the junction. Its value is considered as a figure of merit for a good ohmic contact interface. An ohmic contact is defined as a metal-to-semiconductor contact that has a negligible contact resistance (R_C) relative to the bulk or spreading resistance of the semiconductor. It was shown that the ρ_c is the parameter that controls the contact resistance, its magnitude is important for the device physicists [3, 5].

Many test structures and methodologies are proposed to determine the value of ρ_c of the planar ohmic contacts formed on the heavily doped semiconductor surface [5–10]. However, a direct method of measurement of the specific contact resistance is not possible although the value of specific contact resistance may be evaluated from the measured data obtained from a properly designed test structure (i.e., TLM, Kelvin Resistor, etc). The lay out of the contact resistance test structure for estimating the value of the ρ_c is usually designed according to the TLM concept as proposed by Shockley [5] and further revised by Burger [6] and Reeves et al [7] also offers a convenient method of determining value of the ρ_c, and commonly accepted. Recently, three-point probe (TPP) method based on the extrapolation technique [10] or its revised version [11] also offers a convenient way of determining the specific contact resistance. In all these techniques, the voltage generated (V) for a fixed amount of current injection (I) between the planar ohmic contacts connected by the diffused layer with different length [5–9] or same length [10, 11] is measured, i.e., V/I. This ratio gives the value of the contact resistance R_c (in Ω), from which the value of ρ_c is deduced. Hence, a direct estimation of the ρ_c from the test structure is not possible although it may be estimated by multiplying the measured V/I data with the area of the contact metallization [5, 6]. However, a major drawback of the TLM approach is that the total resistance (R_T) measured consists of not only the resistance of the interfacial layer (R_c), but also the resistance of the diffused layer (R_s) between the contacts and the resistance of the metal layer (R_M) at the contact region. Hence, the measured data might not be reliable. Moreover, in practice, it is difficult to construct a practical sized contact structure that passes a uniform current over its entire area so that the definition of the ρ_c given in the Eq. (1) is considered in the limit as the elemental contact area approaches zero [4–6]. Besides this, these test structures are usually fabricated on the same wafer to monitor a particular process. Therefore, making a test structure requires an additional process steps.

A new non-destructive experimental measurement procedure, namely the iteration technique based on the calculation of the power loss associated with various resistive components of the solar cell normalized to the unit cell area is proposed. It shows that this method can be suitably applied to estimate the value of ρ_c of the screen-printed front Ag thick-film metal contacts of the solar cells. The essential feature of this approach is that no test structure with planar ohmic contacts is required for the measurement purpose than one reported in earlier studies [5–11]. Therefore, it avoids the complexity of making a standard test structure with planar ohmic contacts, but uses a fully finished silicon solar cell. The contact structure consists of Ag thick-film conductor paste deposited by screen-printing technique on the phosphorous doped n^+ silicon surface followed by a thermal annealing step for the contact formation at temperature 600–730 °C for a sintering time of 5–2 min.

2 Experimental

Bright etched 4-inch (100) oriented Cz silicon wafers (p-type, 1Ω-cm) were used to fabricate 10×10 cm^2 solar cells. A cold solution of HF:HNO_3:CH_3–COOH (1:5:1 by volume ratio) is used to bright etch the silicon surface so that the damage created due to the wire sawing during the slicing of the large ingot into the silicon wafers is significantly reduced. This step is followed by a thorough rinse in 18MΩ de-ionized (DI) water. The phosphorous diffusion was carried out at 850 °C using phosphorous oxychloride ($POCl_3$) liquid source in nitrogen-oxygen gas ambient at a flow rate of 40–20 lph respectively. During the diffusion process, the flow rate of the $POCl_3$ source and the pre-deposition time was varied between 15 and 30 min. The sheet resistance of the heavily doped n^+ region was measured using a standard four-point probe method [12] and found to be in the range 10–45Ω/sq. After removing the phosphorous silicate glass (PSG) from the diffused n^+ silicon surface by post diffusion clean in a dilute HF solution, the wafers were thoroughly cleaned in the DI water. The Ag paste was screen-printed on the front surface and fully covered Ag/Al paste on the rear surface. Printing is yielded by respective paste squeezing through the mesh opening in the screen. After screen-printing, both front and rear contacts were dried and annealed at 240 °C to burn off the binders and chemicals added during the screen-printing process. The applied contacts were sintered[1] at temperature varying between 600 and 730 °C in air ambient (i.e., nitrogen-oxygen gas mixture by 3:1 volume ratio at a flow rate of 45 and 15 lph respectively). The presence of oxygen

[1] The term sintering is used to describe as a high temperature annealing step that results in the formation of silicon-metal alloy structure on the heavily doped silicon surface in air ambient condition.

is essential for a good sintering process to occur. Because, it helps to burn off the binders and chemicals in the Ag conductor paste and helps to partially oxidize the silicon surface, thereby forms a thin layer of thermally grown silicon dioxide (SiO_2). This SiO_2 layer is effectively etched by the molten glass-frit during the sintering process and produces a good adhesion to the underlying n^+ silicon surface. The different sintering times were applied for the selected temperature range of 600–730 °C to identify an optimum thermal cycle for studying the peak firing temperature dependent variation of ρ_c of the screen-printed Ag thick-film metal contacts. It helps to assess the electrical nature of the ohmic contacts in terms of specific contact resistance as a function of peak firing temperature of sintering process. Two to four cells were processed for each firing temperature and time setting. It was shown that for the accurate indoor calibration of the photovoltaic conversion efficiency, it is essential for a comparison of results under a standard measurement conditions [13]. In order to compare the cell performance in a comparable manner, a set of standard test condition (STC) has been defined [13, 14]. These are specified as the radiant energy of 1000 W/m^2 with a spectral distribution of the solar energy defined as AM 1.5 Global Spectrum at a cell temperature of 25 °C. The current-voltage characteristics (*I–V*) of the finished solar cells were measured under 100 mW/cm^2 at 25 °C (AM1.5 Global spectrum) [13] using a Tungsten halogen lamp as the light source. The intensity of the lamp is standardized against the short circuit current of a reference screen-printed silicon solar cell of 94 cm^2 area. The photovoltaic parameters of the devices were noted.

3 Results and discussion

In a screen-printed solar cell, ohmic losses are associated with the current traveling through the finite resistance of the metal grids, the metal-to-semiconductor contact resistance, the substrate resistance and the heavily doped emitter region [5, 10, 14, 15]. For a good ohmic contact, a conventional approach to reduce the ohmic losses is to provide a heavily doped region between the metal and the semiconductor region [4, 5]. It is rather simple and reliable to assess both the ohmic losses of the solar cell by quantifying the contribution of the each resistive component to the total power loss of the solar cell. This is done based on the calculation of the relative power loss associated with the current traveling through various resistive components of the solar cell normalized to unit cell area. By meaning the normalized to unit cell area, it is meant that all the individual power loss expressions for the various resistive components are uniformly normalized by dividing with 2nab, the area of the cell [5, 10, 15]. The power loss associated with current traveling through the diffused n^+ emitter region is given by [10],

$$P_{\text{sheet}} = \frac{1}{3} J_L^2 b^2 R_s \tag{2}$$

where J_L is the measured current density of the device corresponding to the maximum power point in the *I–V* characteristics of the cell, R_s is the sheet resistance of the n^+ emitter surface and b is given by $2b = d + L$ (where d is the width of the grid contact and L is the separation between the grid metallization). The power loss associated with the contact resistance for the front Ag metal contact is,

$$P_{\text{fc}} = J_L^2 b[\rho_c R_s]^{1/2} \tag{3}$$

where ρ_c is the specific contact resistance at the interface of the metal and heavily doped semiconductor surface. The power loss associated with the current flow along the front grid finger is given by,

$$P_{\text{finger}} = \frac{2}{3} \frac{J_L^2 a^2 b \rho_f}{t w_b} \tag{4}$$

where a is length of the cell t is the thickness of the grid finger, w_f is the width of the grid fingers and ρ_f is the resistivity of the grid finger material. The power loss associated with the current flow along the busbar is given by,

$$P_{\text{busbar}} = \frac{1}{3} \frac{J_L^2 a n^2 b^2 \rho_f}{t' w} \tag{5}$$

where n is total number of grid fingers and w_b is the average width of the busbar. The current flow through the base region of the cell results in a power loss as given by,

$$P_{\text{base}} = J_L^2 \rho_b l \tag{6}$$

where l is the thickness of the base region of the cell, and ρ_b is the resistivity of the semiconductor base material [10, 16]. As the back contact covers the entire cell area, its contribution to the resistive power loss as calculated is very negligible [10, 15].

From the equation (3), it is seen that the power loss associated with the contact resistance of the front metal contact is related to the specific contact resistance (ρ_c) and sheet resistance (R_s) of the n^+ region underneath the contact window [10, 17]. Therefore, the power loss corresponding to the contact resistance associated with the front Ag contacts (P_{fc}) can be estimated from the total power loss (P_{total}) accordingly,

$$P_{\text{fc}} = P_{\text{total}} - (P_{\text{sheet}} + P_{\text{finger}} + P_{\text{busbar}} + P_{\text{base}}) \tag{7}$$

The measured *I–V* characteristics of the cell were fitted into single exponential model of the current-voltage relationship [14],

$$I = -I_L + I_S\left(\exp\left(\frac{q(V - IR_S)}{nkT}\right) - 1\right) - \left[\frac{V - IR_s}{R_{sh}}\right] \quad (8)$$

where I_L is the light generated current density, I_s is given as the diode reverse saturation current originate from the generation–recombination (G–R) of electron-hole pairs in the neutral region and at the surface of the silicon, n is the ideality factor, R_S is the series resistance, R_{sh} is the shunt resistance, q is the electronic charge, k is the Boltzmann's constant and T is the temperature. By comparing the measured *I–V* curve and theoretical curve at $R_s = 0$ and $R_{sh} = \infty$, it is possible to obtain the relative power loss (corresponding to the maximum power point) associated with the various resistive components of the cell. The difference between the measured *I–V* characteristics and theoretical curve at $R_S = 0$ and $R_{sh} = \infty$ is the net power loss delivered at the maximum power point [10]. This is equivalent to the sum of the R.H.S of Eqs. (2–6) [10, 15, 17]. An algorithm was written and evaluated using equation. (3) by invoking other Eqns. (2, 4–8) to estimate the value ρ_c from the power loss normalized to unit cell area. The measured current density (J_L) corresponding to the maximum power point in the *I–V* characteristics of the solar cell and other geometrical parameters of the contact metallization and device dimensions will serve as the necessary inputs in the entire calculations [10, 16]. The value of other parameters used is: $\rho_f = 7 \times 10^{-6}\Omega$–$cm^2$, t = 0.0014 cm, l = 0.03 cm, w_b = 0.3 cm, w_f = 0.01 cm, $b = (d/L)/2$ = 0.155 cm, a = 10 cm, n = 33 and $\rho_b = 1\Omega$-cm. These values are measured parameters based on the cell geometry and properties of the screen-printed solar cells. Thus, it shows that a reliable value of the specific contact resistance of the planar ohmic contacts formed on the heavily doped n^+silicon surface can be estimated based on an iteration technique using the power loss calculation. Further, it is demonstrated that this methodology avoids the complexity of making the design of any lay out of the standard test structure with planar ohmic contacts.

The sintering process of the front grid metal contacts structure is required to produce a good mechanical adhesion with desired low ohmic losses. This shows that contact structure can be fired at temperature between 500 and 850 °C under proper ambient conditions in an open-tube furnace or in line belt furnace [10, 11, 18–21]. However, the peak firing temperature of the contact sintering process should be below the eutectic temperature of 835 °C for the silver-silicon system in air ambient [22]. It was shown that the firing cycle and the composition of the Ag conductor paste determines the value of the contact resistance which ideally characterize the resistance associated with the metal/semiconductor barrier at the metal and the semiconductor interface [5, 11]. The measured value of ρ_c as a function of the peak firing temperature is given in the Fig. 1. It has a typical variation of ρ_c with increasing temperature. This indicates that with increase in firing temperature, the dissolution etch rate of the silicon surface by the molten glass-frit contained in the Ag conductor paste increases and interacts with the underlying n^+ silicon surface. Upon cooling down, the doped Ag–Si eutectic layer recrystalizes and the silicon sinters concurrently with the interfacial reactions and thus creating an Ag metal/n^+ silicon contact structure [11, 18, 20]. From the same figure, it shows that the optimum peak firing temperature with respect to the ρ_c values is found to 730 °C for a sintering time of 2.15 min. At this combination of thermal cycle, the best of value of ρ_c measured is $1.025 \times 10^{-5}\Omega$–$cm^2$ for the screen-printed Ag thick film ohmic contacts. The measured value of ρ_c is compared with the similar data previously reported in the literature [10, 23–25]. The value of $\rho_c \cong 1.01 \times 10^{-3}$ Ω–cm^2 is reported for the screen-printed Ag paste fired in a lamp heated belt in-line furnace [23]. There have been reports of $\rho_c \cong 2.5 \times 10^{-3}$ Ω–cm^2 for the rapidly thermal fired Ag contacts [24, 25] and ~ 14.6×10^{-3} Ω–cm^2 contacts fired in a conventional open-tube furnace [10]. Therefore, the specific contact resistance data obtained in the present study is two or three orders of magnitude lower than the ρ_c data reported earlier for the screen-printed Ag thick-film metal contacts [10, 24, 25]. However, for a good ohmic contact, value of ρ_c of the order of or below 1.0×10^{-6} Ω–cm^2 is required The resistivity of the fired silver grid fingers was supposed to be less than 4.0×10^{-6} Ω-cm [4, 26–27]. This is

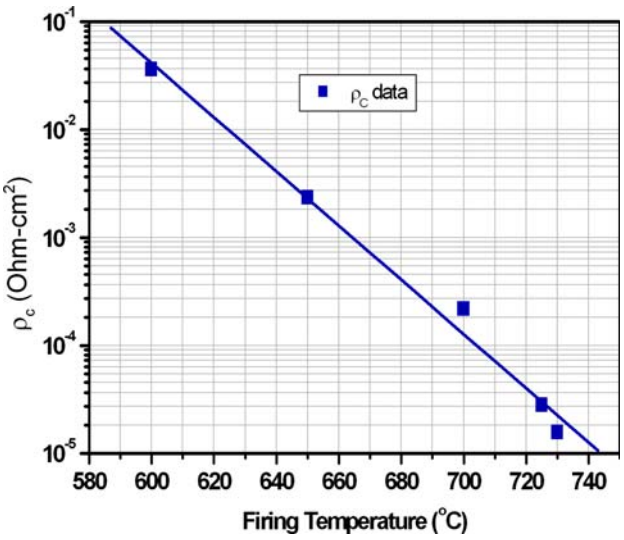

Fig. 1 The dependence of the peak firing temperature of the sintering process on the specific contact resistance of the screen-printed Ag thick-film metal contacts of the solar cells

much less than the electrical resistance of the base region [4]. Therefore, the value of specific contact resistance of the order of $\cong 1.0 \times 10^{-5}$ Ω-cm^2 is reasonably a low value which found to give low ohmic losses in the screen-printed Ag ohmic contact structure formed on the heavily doped silicon surface [10, 17].

The results in the figure 1 shows that the lowest value of the specific contact resistance was obtained when the Ag metal/n$^+$ silicon contact structure was sintered at a optimum firing temperature of 730 °C for a sintering time of 2.15 min. Figure 2 shows the typical example of the variation of the specific contact resistance for the screen-printed Ag thick-film contacts as a function of the sheet resistance (R_{sheet}) of the n$^+$ emitter region of the solar cell. From the figure, it shows that an order of magnitude change in the surface doping concentration (N_S) results nearly two orders of magnitude change in the value of specific contact resistance. This change in the specific contact resistance is resulted from the same orders of magnitude change in the value of contact resistance associated with the Ag metal and n$^+$ silicon contact structure. This result shows that the specific contact resistance has a decreasing trend with increasing in the surface doping concentration. Since the work function of the metal does not appreciably change for different contact systems due to the Fermi level pinning [4, 28], the surface doping concentration is the dominant factor in deciding the value of ρ_c for the planar ohmic contacts. However, the maximum concentration of the dopant that can be dissolved in silicon under equilibrium condition without forming a separate phase is limited by the solid solubility of the dopant in the silicon [29]. If the semiconductor doping is very high, i.e., $N_S \gg 10^{19}$ atoms/cm^3, the depletion region width is so thin that carriers can tunnel through this barrier height. Then, the current transport is dominated by the tunneling of charge carriers across this thin barrier. This additive component of the current flow makes the current-voltage characteristics linear over a large current range, thus giving rise to an ohmic behavior [4]. In such case, the dependence of the specific contact resistance at the metal and the semiconductor contact structure is determined by the surface doping concentration (N_S) and the barrier height (Φ_B) [26, 27],

$$\rho_c = \rho_{C0} \exp\left(\frac{C_1 \Phi_B}{\sqrt{N_S}}\right) \tag{9}$$

where ρ_{C0} is the specific contact resistance for the infinite active surface doping concentration; C_1 is a constant ($\cong 7.0 \times 10^{10}$cm$^{-3/2}$ eV^{-1} for silicon), N_S is the actual surface doping concentration and Φ_B is the barrier height between the metal and the semiconductor [28]. The above equation shows that in the tunneling regime [4, 26–27], the specific contact resistance is strongly depends on the surface doping concentration and exponentially varies with the factor, $\Phi_B/N_S^{1/2}$.The results shown in the Fig. 2 reveals that the value of specific contact resistance is found to be a strong function of the phosphorous doping concentration and follows a linear relationship as predicted by the Eq. (9). The measured sheet resistance of the n$^+$ silicon region can be correlated with surface doping concentration accordingly [12],

$$R_{sheet} = \frac{1}{q\mu N_S t} \tag{10}$$

where q is the electronic charge, μ is the mobility and t is the thickness of the semiconductor layer.

It was found that the glass-frit contained in the Ag conductor paste plays most important role during contact formation. At temperature typically above 600 °C, glass frit particles become fluid and wet the underlying natural silicon dioxide (SiO_2) layer [18, 19, 21]. The glass-frit in the molten state is highly reactive. It etches and penetrates the dielectric SiO_2 layer leading to interact with the silicon, which follows a redox reaction between the lead oxide and silicon [19]. In this process, some amount of the silver and silicon were also dissolved in the lead-silver melt. The Ag metal diffuses only part of the way through the silicon [11, 22]. On cooling down, the silicon epitaxially recrystalizes to form $AgSi_2$. Thus, it results the formation of nearly perfect silver-silicon contact at temperature below the silver-silicon eutectic [11, 18, 20]. The silver crystallite seems to be indispensable for providing a current path from the emitter into the bulk of the Ag thick-film finger [18]. Most of the crystals are separated from the bulk of the silver finger by a glass-frit, which also plays an important role in the current transport [21]. This indicates that rapid

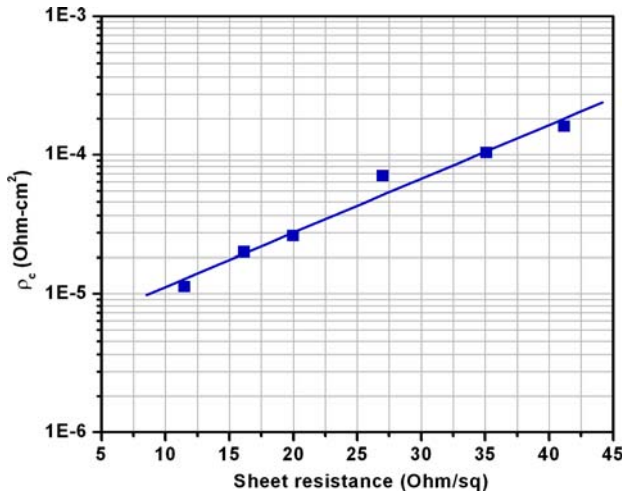

Fig. 2 The dependence of specific contact resistance as a function of the sheet resistance of the heavily n$^+$ emitter region of the silicon surface. The specific contact resistance measured using the iteration technique based on the calculation of power loss

firing is occurring due to the non-uniform annealing of the front Ag thick-film conductor paste, which may affect the electrical nature of the Ag metal/n^+ silicon contact structure [11]. The SEM measurements of the fired Ag contact shows that even if the contacts are fired at an optimum temperature, it does not produce a uniform interfacial region at the metal-to-semiconductor interface [16, 30]. But it creates steps or some irregularities at the interface, micropores and the voids in the sintered Ag contacts due to the fast etch rate of the molten glass-frit with the silicon and the fast ramp rate, etc [11, 30, 31].

4 Conclusions

It is demonstrated that a reliable value of specific contact resistance of the screen-printed front Ag thick-film contacts on the silicon solar cells can be estimated using a newly proposed iteration method. It is basically consists of extracting the value of specific contact resistance by using the calculation of relative power loss associated with the current traveling through various resistive components of the solar cell normalized to unit cell area and the current voltage characteristics of the solar cell. The main advantage of this methodology is that it does not have to use any design lay out of a standard test structure with planar ohmic contacts for the measurement purpose. Thus, it avoids the complexity of making a standard test structure. The result showed that value of ρ_c of the order of 1.0×10^{-5} Ω-cm^2 is obtained for the Ag thick film contacts on the heavily doped silicon. This value is much lower than the ρ_c data previously reported. It is found that a peak firing temperature of 730 °C for 2.15 min is found to give a lower value of $\rho_c \cong 1.0 \times 10^{-5} \Omega$-cm^2 for the front Ag thick-film contacts. The study is further extended to understand the mechanism of contact formation and dependence of the peak firing temperature on the specific contact resistance.

References

1. P. Doshi, J. Meija, K. Tate, A. Rohatgi, IEEE Trans. Electron Devices. **ED-44**(9), 1417–1423 (1997)
2. P.N. Vinod, B.C. Chakravarty, L. Mohan, S.N. Singh, Proceeding of the X International Workshop on the Semiconductor Devices (IWPSD) (Narosa Publications (New Delhi), IIT Delhi, New Delhi, 1999), pp. 1245–1250, Dec 13–17
3. W. Shockley, Report No. AL-TOR-64-207, Air Force Avionics Laboratory, Wright Patterson, Air Force Base, Ohio, USA, September (1964)
4. S.M. Sze, *Physics of the Semiconductor Devices* (Wiley, NY, 1981)
5. D.L. Meier, D.K. Schroder, IEEE Trans. Electron Devices. **ED-31**, 647–653 (1984)
6. H.H. Berger, J. Electrochem. Soc. **119**, 507–514 April (1972); H.H. Berger, Solid State Electronics **15**, 145–158
7. G.K. Reeves, H.B. Harrison, IEEE Trans. Electron Device Lett. **EDL-18**(25), 1083–1085 (1982)
8. S.J. Procter, L.W. Lindholm, J.A. Maze, IEEE Trans. Electron Devices, **ED-30**, 1535–1542 (1983)
9. J. Chen, W.L. Oldham, IEEE Trans. Electron Device Lett. **EDL-5**, 178–180 May (1984)
10. P.N. Vinod, B.C. Chakravarty, K. Ravi, L. Mohan, S.N. Singh, Semiconductor Sci. Technol. **15**, 286–290 (2000)
11. P.N. Vinod, Semiconductor Sci. Technol. **16**, 966–971 (2005).
12. F.M. Smits, Bell System Tech. J. **37**, 711–718 (1958).
13. M.A. Green, *High Efficiency Silicon Solar Cells* (Trans Tech Publications, Switzerland 1987)
14. A.G. Aberle, S.R. Wenham, M.A. Green, Proc. 23rd IEEE Photovoltaic Specialists Conference (PVSC) (IEEE New York Inc., 1993) pp. 133–137
15. S. Silvestre, D. Patron, L. Castener, P. Ashburn Proc. 25th IEEE Photovoltaic Specialists Conference (PVSC) (Washington DC, P. 497, IEEE, New York, 1996)
16. P.N. Vinod, Ph.D Thesis. University of Delhi, India, (2003)
17. D.K. Schroder, D.L. Meier, IEEE Trans. Electron Devices **ED-31**, 637–647 (1984)
18. C. Ballif, D.M. Huljic, G. Willeke, A. Hessler-Wyser, Appl. Phys. Lett. **82**(12), 1878–1880 (2003)
19. G. Schubert, B. Fischer, P. Fath, Proc. Photovoltaics in Europe Conf, Rome, pp. 343–346 (2002)
20. C. Ballif, D.M. Huljic, A. Hessler-Wyser, G. Willeke, Proc. 29th IEEE Photovoltaic Specialists Conference (PVSC) (Glasgow, U.K, 2002), pp. 360–363
21. G. Schubert, F. Huster, P. Fath, Proc. 14th Photovoltaic Solar Energy Convention (PVSEC) (Bangkok, Thailand, 2004), pp. 441–445
22. R.W. Olesinski, G.K. Abbaschian, in *Binary Alloy Phase Diagrams*, 2nd edn. ed. by T.B. Massalski, (1–3 American Society for Metals, Metals Park, Ohio, USA, 1992)
23. M.M. Halili, A. Rohatgi, C. Khadikar, S. Kim, J. Pham, S. Salami, A. Sheikh, S. Sridharan, in *Proc. European Council Photovoltaic Solar Energy Conf (EC PCSEC), 7–11 June* (Paris, France, 2004), pp. 1300–1303
24. B. Thuillier, S. Berger, J.P. Boyeaux, A. Laugier, Proc. 28th IEEE Photovoltaic Specialists Conf (PVSC) (Anchorage, 2000), pp. 411–413
25. G. Grupp, D.M. Huljic, R. Prue, G. Willeke, J. Luther, Proc. 20th European Photovoltaic Solar Energy Conference And Exhibition (EC PVSEC) (Barcelona, Spain, 6–10 June, 2005)
26. C.Y. Chang, Y.K. Fang, S.M. Sze, Solid State Electronics **14**, 541–550 (1972)
27. C.M. Osborn, K.R. Bellur, Thin Solid Films **332**, 428–436 Nov (1998)
28. M.S. Tyagi, *Introduction of Semiconductor Physics and Devices* (Wiley, 2002)
29. F.A. Trumbore, Bell System Tech J **37**, 205–218 (1960); J.D. Plummer, P.B. Griffin, Proc. of IEEE **89**(3), 240–258, April (2001)
30. B.C. Chakravarty, B.K. Das, S.N. Singh, S.K. Sharma, S.U.M. Rao, R. Kumar, B.R. Chakravarty, J. Mat. Sci. Lett. **12**, 447–451 (1993)
31. S.B. Rane, T. Seth, G.J. Phatak, D.P. Amelneker, J. Mat. Sci. Mat. Electronics **15**, 103–106 (2004)